

# Dynamics of Non-Canonical Amino Acid-Labeled Intra- and Extracellular **Proteins in the Developing Mouse**

Aya M. Saleh, Kathryn R. Jacobson, Tamara L. Kinzer-Ursem, and Sarah Calve (b)

Weldon School of Biomedical Engineering, Purdue University, 206 South Martin Jischke Drive, West Lafayette, IN 47907, USA

(Received 5 March 2019; accepted 17 August 2019; published online 26 August 2019)

Associate Editor Stephanie Michelle Willerth oversaw the review of this article.

#### Abstract

Introduction-Mapping protein synthesis and turnover during development will provide insight into functional tissue assembly; however, quantitative in vivo characterization has been hindered by a lack of tools. To address this gap, we previously demonstrated murine embryos can be labeled with the non-canonical amino acid azidohomoalanine (Aha), which enables the enrichment and identification of newly synthesized proteins. Using this technique, we now show how protein turnover varies as a function of both time and cellular compartment during murine development.

Methods-Pregnant C57BL/6 mice were injected with Aha or PBS (control) at different embryonic time points. Ahalabeled proteins from homogenized E12.5 and E15.5 embryos were conjugated with diazo biotin-alkyne, bound to Neu-

Address correspondence to Sarah Calve, Weldon School of Biomedical Engineering, Purdue University, 206 South Martin Jischke Drive, West Lafayette, IN 47907, USA. Electronic mail: scalve@purdue.edu

Sarah Calve received her B.S. in Materials Science and Engineering from Cornell University, then a M.S. in Molecular, Cellular and Developmental Biology and a Ph.D. in Macromolecular Science and Engineering from the University of Michigan. Her doctoral research focused on the design and mechanical characterization of self-assembling constructs for musculoskeletal repair, under the guidance of Prof. Ellen Arruda. As a postdoctoral fellow at Northwestern University's Children's Memorial Hospital, Sarah investigated the role of extracellular matrix remodeling during newt limb regeneration. Sarah joined the Weldon School of Biomedical Engineering at Purdue University as an assistant professor in 2012. Her research group, the Musculoskeletal Extracellular Matrix Laboratory, is actively developing tools to quantify how the composition, turnover, organization and mechanical properties of the musculoskeletal system change during scar-free tissue assembly. The goal is to use these tools to elucidate how different components integrate to form functional tissues during normal development and identify parameters that will guide the design of regenerative therapies. In 2017, she became the first Purdue professor to receive the NIH Director's New Innovator Award. Additional recognitions include the BMES-CMBE Rising Star Junior Faculty Award (2018), inclusion in the National Academy of Engineering, Japan-America Frontiers of Engineering Symposium (2018) and being named the Leslie A. Geddes Assistant Professor of Biomedical Engineering at Purdue (2019).

This article is part of the CMBE 2019 Young Innovators special

trAvidin beads, selectively released, then processed for either SDS-PAGE or LC-MS/MS. For turnover studies, embryos were harvested 0–48 h after Aha injection at E12.5, separated into different cellular fractions based on solubility, and analyzed via western blotting.

Results—We developed an enhanced method for isolating Aha-labeled proteins from embryos that minimizes background signal from unlabeled proteins and avidin contamination. Approximately 50% of all identified proteins were found only in Aha samples. Comparing proteins present in both Aha and PBS samples, 90% were > 2-fold enriched in Aha-treated embryos. Furthermore, this method could resolve differences in the Aha-labeled proteome between developmental time points. Newly synthesized Aha-labeled proteins were observed by 3 h and peak labeling was around 6 h. Notably, extracellular matrix and cytoskeletal turnover appeared lower than the cytosolic fraction.

Conclusions—The methods developed in this work enable the identification and quantification of protein synthesis and turnover in different tissue fractions during development. This will provide insight into functional tissue assembly and ultimately inform the design of regenerative therapies that seek to promote growth and repair.

Keywords-BONCAT, Azidohomoalanine, Diazo biotinalkyne, Click chemistry, Mass spectrometry.

## **ABBREVIATIONS**

| ACN   | Acetonitrile               |
|-------|----------------------------|
| AG    | Aminoguanidine             |
| Aha   | Azidohomoalanine           |
| C     | Cytosolic                  |
| CS    | Cytoskeletal               |
| CuAAC | Copper(I)-catalyzed azide- |
|       | alkyne cycloaddition       |
| DBA   | Diazo biotin-alkyne        |
| DTT   | Dithiothreitol             |
| ECM   | Extracellular matrix       |
| FA    | Formic acid                |
| FDR   | False discovery rate       |
| GO    | Gene ontology              |
|       |                            |

HPLC High performance liquid chromatography

LC-MS/MS Liquid chromatography-tandem

mass spectrometry

LFQ Label-free quantification

M Membrane Met Methionine

MS Mass spectrometry

N Nuclear

Na<sub>2</sub>S<sub>2</sub>O<sub>4</sub> Sodium dithionite NaAsc Sodium ascorbate

ncAA Non-canonical amino acid

QE HF Q exactive HF hybrid quadrupole-

orbitrap mass spectrometer

SDS Sodium dodecyl sulfate

SDS-PAGE Sodium dodecyl sulfate-polyacrylamide

gel electrophoresis

SILAC Stable isotope labeling by amino

acids in cell culture

TBS Tris-buffered saline TFA Trifluoroacetic acid

THPTA Tris(3-hydroxypropyltriazolyl-

methyl)amine

#### INTRODUCTION

During functional tissue assembly, temporal activation of intracellular protein signaling pathways drive cell division, motility and differentiation, and the surrounding extracellular matrix (ECM) is remodeled to provide cues and support for these cellular processes. However, little is known regarding the synthesis and turnover of proteins in different cellular compartments during the scar-free formation of tissues (i.e. during development, repair and regeneration). This information is critical for providing benchmarks for regenerative medicine; only by identifying the dynamics of intra- and extracellular proteins that drive native tissue assembly can therapies that better restore functionality to damaged tissues be designed.

Developmental model systems are ideal for studying the role of proteins in the de novo formation of tissues. Liquid chromatography–tandem mass spectrometry (LC–MS/MS), which enables the identification of proteins within complex samples, has been used to investigate development in *D. melanogaster*, *Y. laevis*, and *D. rerio*, 25,32 as well as single time point studies of rat embryonic heart 3 and embryonic murine tissue. More recently, a comprehensive study comparing the proteome and transcriptome of the developing murine stomach was conducted 1; but these investigations typically focused on unfractionated tissue lysates, which consequently leads to the domina-

tion of the MS spectra by proteins that are in higher abundance. This is a critical bottleneck in identifying proteins within developing tissues since proteins of varying solubility are spread across different cellular compartments (i.e. cytosolic, membrane, nuclear, cytoskeletal and matrisome or ECM), and many will not be identified using a single extraction method. To increase the coverage of proteins within complex tissues, buffers of different ionic strength and detergent composition can be used to selectively fractionate proteins. Researchers have used these fractionation methods to characterize the composition and turnover of different cellular compartments of various healthy and pathological adult tissues 12,14,20,23,38,47,52; however, the dynamics of both intra- and extracellular proteins during mammalian embryogenesis remains largely unknown.

LC-MS/MS-based analyses can reveal protein turnover rates through stable isotope labeling by amino acids in cell culture (SILAC).<sup>3,10,20</sup> Unfortunately, it is necessary to feed animals a diet containing isotope-labeled amino acids for prolonged periods to achieve complete proteome labeling.<sup>35</sup> Additional limitations of SILAC labeling are that proteins in low abundance are often undetected and it is not possible to specifically isolate or tag SILAC-labeled molecules.<sup>3</sup>

To address the insensitivity of isotope labeling for newly synthesized proteins, non-canonical amino acid (ncAA) labeling was developed for selective analysis of de novo protein synthesis.<sup>17</sup> In this method, cells are cultured in media supplied with a methionine (Met; Fig. 1a) analog such as azidohomoalanine (Aha; Fig. 1a), which possesses an azide moiety. Due to the structural similarity to Met, cells incorporate Aha into growing protein chains using the endogenous translational machinery.<sup>27</sup> As a result, new proteins synthesized during pulse labeling with Aha are tagged with azides. 17 Importantly, azides are a bioorthogonal chemical group, meaning that they are biocompatible but do not cross-react with native biological systems and can be selectively modified through specific chemical reactions.<sup>5</sup> Azides can be conjugated to alkynes, forming a stable triazole product, using copper(I)-catalyzed azide-alkyne cycloaddition (CuAAC; Fig. 1a), also known as a "click" chemistry reaction. 43 Accordingly, the newly synthesized Aha-labeled proteins can be either ligated to affinity tags for selective enrichment and identification or fluorescent molecules for protein tracking and visualization. 15-17,26

Over the last decade, ncAA labeling has been applied to various bacterial and mammalian cell culture systems *in vitro* to study biological processes ranging from quorum sensing to inflammation. <sup>46</sup> Importantly, Bagert *et al.* demonstrated that ncAA labeling can be applied to resolve protein synthesis



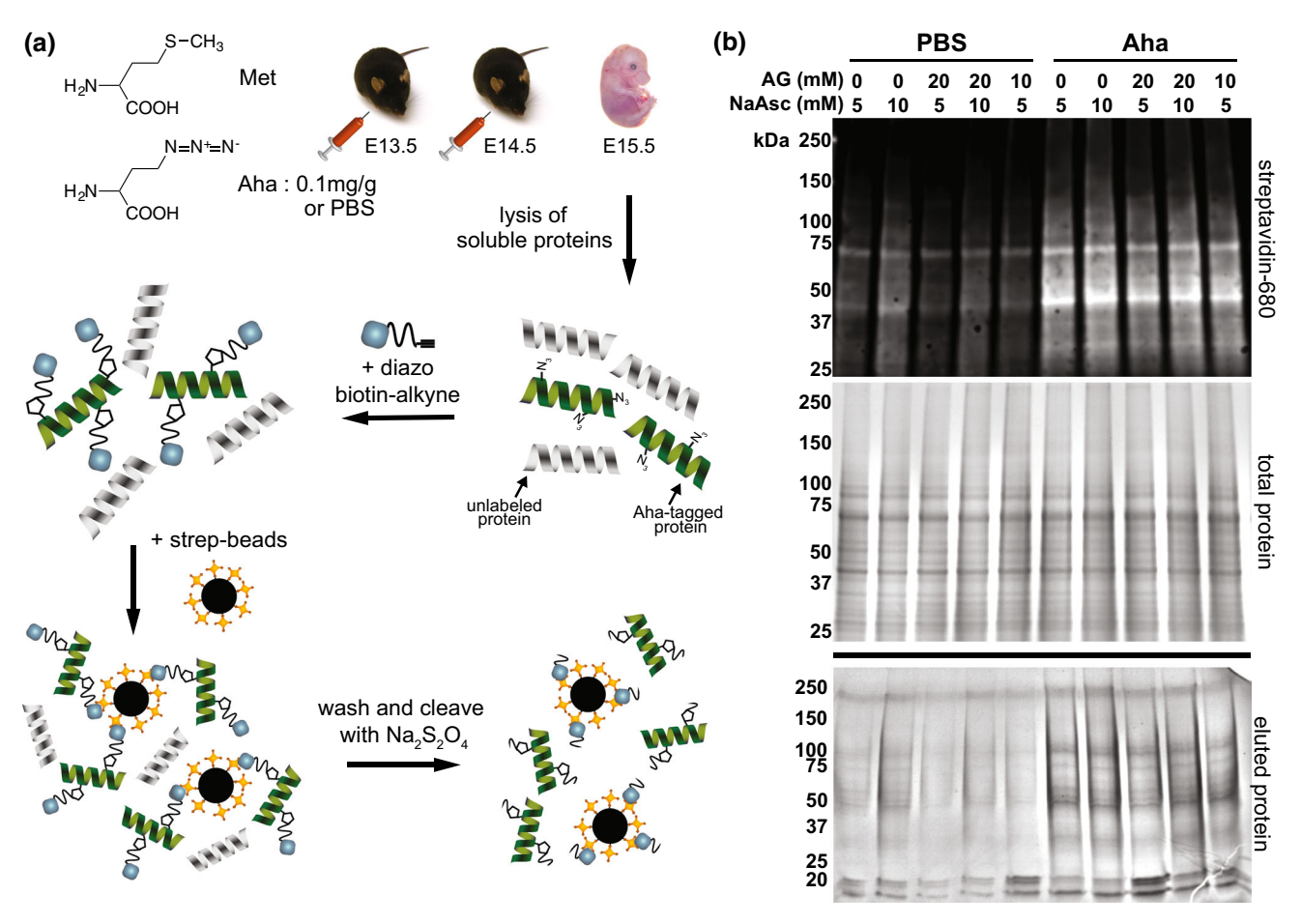


FIGURE 1. Enrichment of Aha-labeled proteins from murine embryos. (a) Workflow for enrichment of Aha-labeled proteins using a diazo biotin-alkyne (DBA) linker. The methionine (Met) analog, azidohomoalanine (Aha), was injected into time-mated dams at 0.1 mg/g, once a day at E13.5 and E14.5, whereas 10  $\mu$ L/g PBS was injected into control animals. E15.5 embryos were harvested and lysates of soluble proteins were reacted with DBA and isolated using NeutrAvidin beads. Unlabeled proteins were washed away and Aha-labeled proteins were released using Na<sub>2</sub>S<sub>2</sub>O<sub>4</sub>. (b) Soluble lysates from E15.5 embryos generated as described in (a) were reacted with DBA using different concentrations of sodium ascorbate (NaAsc) and aminoguanidine (AG). Lysates (18.5  $\mu$ g/well) were analyzed *via* western blotting (top) to confirm Aha labeling, a duplicate gel was run at the same time to ensure equal loading (middle, Coomassie-stained gel). The same samples were enriched using the workflow in (a) and eluted proteins were run on a gel and stained with Coomassie (bottom). NaAsc increases nonspecific binding of unlabeled proteins to NeutrAvidin beads (see also Fig. S1c), whereas addition of AG reduces the nonspecific binding.

within narrow time intervals.<sup>3</sup> Given the limitations of in vitro cell culture, extending the studies to the more complex in vivo environment is essential to augment our understanding of the dynamics of protein synthesis. McClatchy et al. first showed that in vivo labeling of the murine proteome is feasible by feeding animals an Aha-enriched diet for several days. 36 More recently, our group developed an injection-based technique that enables global labeling of murine proteome with ncAAs.8 Our results demonstrated that two days of intraperitoneal injection of Aha was sufficient for systemic incorporation of Met analogs into the proteome of both juvenile mice and developing embryos with no overt perturbation of physiological functions. Our method provides several advantages over introducing ncAAs or stable isotopes in the animal diet including: ease of intraperitoneal or subcutaneous

injection, global proteome labeling in a shorter time period, and more accurate dose–effect calculations.

The successful incorporation of ncAAs into the murine proteome through direct injection provides us with the opportunity to use a developmental model to temporally and spatially probe protein dynamics. However, to resolve dynamics of different intra- and extracellular proteins in the developing embryo, it is first necessary to generate a method that combines ncAA labeling and cellular compartment fractionation. The goals of this study were to build upon our previous results and (1) optimize ncAA enrichment for newly synthesized proteins in murine embryos, (2) demonstrate this technique could resolve differences in the proteomes of embryonic time points, (3) utilize a tissue fractionation technique to isolate embryonic intra- and extracellular proteins and (4) combine ncAA labeling



and tissue fractionation techniques to investigate turnover of different cellular compartments in developing embryos.

Using a cleavable biotin-alkyne linker, we could substantially enrich for Aha-labeled proteins from murine embryos compared with unlabeled controls. Identification of Aha-labeled proteins via LC-MS/MS showed that there was a significant difference in the composition of newly synthesized proteins from Ahatreated E12.5 and E15.5 embryos. The complexity of individual samples was reduced when proteins were fractionated into different cellular compartments. Importantly, we showed the dynamics of Aha-labeling in the murine embryo varied as a function of time and cellular compartment. With these tools in hand, we are now poised to conduct a more comprehensive temporal analysis of synthesis and turnover for various intraand extracellular proteins. Quantification of protein turnover is critical for understanding development, homeostasis and disease progression, and this method has the potential to determine the cues necessary for the formation and maintenance of functional tissues.

#### MATERIALS AND METHODS

Unless otherwise specified, all reagents were of chemical grade from Sigma-Aldrich (St. Louis, MO) and reagent stock solutions were made with HPLC-grade water.

## Animal Model

Animals used in these studies were derived from wild-type C57BL/6 mice (Mus musculus) purchased from The Jackson Laboratory. All experimental protocols were performed in compliance with established guidelines and all methods were approved by Purdue Animal Care and Use Committee (PACUC, protocols# 1209000723 and 1801001682). PACUC requires that all animal programs, procedures, and facilities at Purdue University to abide by the policies, recommendations, guidelines, and regulations of the USDA and the United States Public Health Service in accordance with the Animal Welfare Act and Purdue's Animal Welfare Assurance. To generate embryos of defined ages, female mice were time-mated with males and noon on the date when a copulation plug was found was considered to be embryonic day (E)0.5.

#### Aha Labeling and Embryonic Tissue Collection

The methionine (Met; Fig. 1a) analog L-azidohomoalanine (Aha; Fig. 1a, Click Chemistry Tools, Scottsdale, AZ) was resuspended in phosphate buf-



fered saline (PBS; 10 mg/mL), pH adjusted to 7.4 with NaOH, sterile filtered and stored at  $-20\,^{\circ}\text{C}$ . All injections were administered to pregnant dams subcutaneously at 0.1 mg/g Aha and sterile PBS was used for control injections at 10  $\mu$ L/g mouse. Embryos were collected at the desired time after injection by euthanizing dams via CO<sub>2</sub> inhalation, which was confirmed using cervical dislocation. The uterine horns were removed and dissected in ice cold PBS, then embryos were snap frozen in liquid nitrogen and stored at  $-80\,^{\circ}\text{C}$ .

## Optimization of Aha Enrichment

Pregnant females were injected with Aha or PBS once a day for two days, and embryos were harvested 24 h after the last injection (E12.5 or E15.5). For E12.5, three embryos were pooled for each biological replicate, whereas a single E15.5 embryo was used per biological replicate (n = 3), homogenized in ice cold lysis buffer [PBS (pH 7.4) with 0.3% sodium dodecyl sulfate (SDS), 1 × protease inhibitors (ThermoFisher Scientific, Waltham, MA) and 45 U benzonase (EMD Millipore, Darmstadt, Germany)] using a TissueRuptor (Qiagen, Venlo, Netherlands). Homogenates were rotated end-over-end at 4 °C for 1 h and then cleared by centrifugation at  $21,100 \times g$  for 20 min. Protein concentration of cleared lysates was determined using the Pierce 660 nm Protein Assay (ThermoFisher Scientific). Lysates were alkylated with 30 mM iodoacetamide for 1 h at room temperature (RT) protected from light. The alkylated lysates were then reacted with diazo biotin-alkyne (DBA; Fig. S1; Click Chemistry Tools) in a copper-catalyzed azide-alkyne cycloaddition (CuAAC) reaction with [50 µM DBA, 5 mM tris(3-hydroxypropyltriazolylmethyl)amine (THPTA; Click Chemistry Tools), 1 mM CuSO<sub>4</sub>, 0-20 mM aminoguanidine (AG) and 5 or 10 mM sodium ascorbate (NaAsc)] in a reaction volume of 800 μL with a final protein concentration of 2.5 mg/mL. The samples were rotated end-over-end at 4 °C overnight and excess unreacted DBA was removed using Zeba Spin Desalting Columns, 7 K MWCO (ThermoFisher Scientific). Desalted samples were supplemented with 1% NP-40 and Aha-labeled proteins were affinity purified by incubation with 100 μL settled NeutrAvidin agarose beads (ThermoFisher Scientific) for 1.25 h with end-over-end mixing at 4 °C. The beads were then washed four times with 1 mL (10  $\times$  bead volume) PBS (pH 7.4) containing 0.05% SDS and 1% NP-40 to remove unlabeled proteins. Aha-labeled proteins were eluted by incubating beads with 400  $\mu$ L elution buffer [PBS (pH 7.2), 100 mM Na<sub>2</sub>S<sub>2</sub>O<sub>4</sub>, 0.05% SDS] for 1 h at RT, protected from light. Eluted proteins were precipitated by adding 1.6 mL 100% acetone (4 × elution volume) and incubating overnight at -20 °C. Proteins were pelleted by centrifugation for 20 min at  $21,100 \times g$  and washed by adding 1.6 mL 80% acetone and incubating for 1.5 h at -20 °C. Samples were pelleted and dried at 26 °C in a centrivap concentrator (Labconco, Kansas City, MO) for 20 min and processed for LC-MS/MS as described below.

## Western Blot Analysis of Aha-Labeled Samples

Proteins were resolved on 4–20% SDS-PAGE gels (BioRad, Hercules, CA) for 37 min at 170 V, transferred to a PVDF membrane (ThermoFisher Scientific) using a semi-dry transfer system for 40 min and probed overnight at 4 °C with IRDye 680 Streptavidin (LICOR, Lincoln, NE) diluted 1:3000 in Tris-buffered saline (TBS) with 0.05% Tween 20 + Protein-Free TBS Blocking Buffer (ThermoFisher Scientific) at a ratio of 1:1. Membranes were imaged using an Azure Biosystems c600 and then stained with Ponceau S (Sigma-Aldrich) for 20 min to confirm equal protein loading.

# LC-MS/MS Analysis of Aha-Enriched Samples

Pellets were suspended in 50 µL 8 M urea with 100 mM ammonium bicarbonate. Proteins were reduced with 10 mM dithiothreitol (DTT) for 2 h at 37 °C, shaking at 1000 rpm (Eppendorf ThermoMixer F1.5, Hauppauge, NY). Samples were cooled to RT and alkylated with 25 mM iodoacetamide for 30 min while protected from light. Each sample was diluted with 100 mM ammonium bicarbonate to a final concentration of 2 M urea. Samples then underwent three subsequent digestion steps, all at 37 °C and constant shaking at 1000 rpm: (1) 2 h with 1  $\mu$ g/200  $\mu$ L Endoproteinase LysC (New England Biolabs, Ipswich, MA); (2) overnight with  $3 \mu g/200 \mu L$  trypsin (MSgrade, ThermoFisher Scientific); and (3) an additional 2 h with 1.5  $\mu$ g/200  $\mu$ L trypsin. Afterwards, enzymes were inactivated with 0.1% trifluoroacetic acid (TFA; VWR, Radnor, PA).

Peptides were processed with Pierce Detergent Removal Spin Columns (ThermoFisher Scientific) per the manufacturer's protocol. Samples were incubated on the column resin for 2 min prior to centrifugation for 2 min at  $1500 \times g$ . Following detergent removal, samples were cleaned of excess salts with C-18 MicroSpin Columns (The Nest Group Inc., Southborough, MA). Briefly, columns were conditioned with  $100 \mu L$  100% acetonitrile (ACN; ThermoFisher Scientific) and equilibrated with  $100 \mu L$  0.1% TFA. Samples were added to the C-18 columns, washed with  $300 \mu L$  0.1% TFA, and eluted in  $100 \mu L$  80% ACN with 25 mM formic acid (FA; ThermoFisher Scientific). Peptides

were dried for 4 h at 45 °C in a centrivap concentrator and suspended in 10  $\mu$ L of 3% ACN with 0.1% FA. After suspension, peptide concentration was measured with the Pierce Quantitative Colorimetric Peptide Assay (ThermoFisher Scientific) and the most concentrated Aha sample was brought to 0.2  $\mu$ g/ $\mu$ L by addition of 3% ACN with 0.1% FA. The equivalent volume of 3% ACN with 0.1% FA was added to remaining Aha and PBS samples. Samples were stored at -80 °C until analyzed using LC–MS/MS.

Peptides were analyzed using the Dionex UltiMate 3000 RSLC Nano System coupled to the Q exactive HF hybrid quadrupole-orbitrap mass spectrometer (QE HF; ThermoFisher Scientific). Following digestion, 1  $\mu$ g of peptide was loaded onto a 300  $\mu$ m i.d. × 5 mm C18 PepMap 100 trap column and washed for 5 min using 2% ACN with 0.01% FA at a flow rate of 5  $\mu$ L/min. After washing, the trap column was switched in-line with a 75  $\mu$ m  $\times$  50 cm reverse phase Acclaim C18 PepMap 100 analytical column heated to 50 °C. Peptides were separated using a 120min gradient elution method at a flow rate of 300 nL/ min. Mobile phase A consisted of 0.01% FA in purified water, while mobile phase B consisted of 0.01% FA in 80% ACN. The linear gradient started at 2% B and reached 10% B in 5 min, 30% B in 80 min, 45% B in 91 min, and 100% B in 93 min. The column was held at 100% B for the next 5 min before being brought back to 2% B and held for 20 min. Samples were injected into the QE HF through the Nanospray Flex Ion Source fitted with an emission tip from New Objective. Data acquisition was performed monitoring the top 20 precursors at 120,000 resolution with an injection time of 100 ms.

## Analysis of LC-MS/MS Spectra

Raw data files were analyzed using MaxQuant (version 1.6.1.0). Default settings were used unless noted otherwise (see all parameters in Table S1). Peak lists were searched against the Mus musculus Uniprot FASTA database (November 2018), Gallus gallus Avidin Uniprot FASTA protein sequence (May 2018) and a common contaminants database (January 2018). Cysteine carbamidomethylation was included as a fixed modification as were pertinent variable modifications (Table S1). Peptide and protein false discovery rates (FDR) were set to 0.01 and determined by a reverse decoy database derived from the Mus musculus database. Raw protein intensities were analyzed with Microsoft Excel (for filtering and data handling) and GraphPad Prism 8 (for data visualization). Proteins that had less than two razor and unique peptides or proteins marked as a potential contaminant or reverse hit were removed. In addition, proteins identified by



match between runs were removed prior to analysis. Proteins were only included in subsequent analyses if identified in at least two biological replicates. Raw intensities were  $\log_2$  transformed and were considered enriched if  $[\log_2(Aha \text{ raw intensity}) - \log_2(PBS \text{ raw intensity})] > 1$  (indicating a > 2-fold change). Tissue compartment categories (cytosolic, nuclear, membrane, cytoskeletal, matrisome) were assigned to proteins using categorizations derived from the Gene Ontology (GO) Consortium<sup>2</sup> and The Matrisome Project. The Matrisome Project. Percentage of each category was calculated by dividing the summed protein intensities designated to the given compartment by the total protein intensity in the sample.

To compare the distribution of Aha-labeled proteins identified in E12.5 and E15.5 embryos, the raw intensities were normalized and visualized using a volcano plot. All raw intensities in individual samples were summed, then averaged over biological replicates for each time point and a normalization factor was generated by dividing the average raw intensity of E12.5 by E15.5. The raw intensity of each protein in E15.5 samples was multiplied by the normalization factor and  $\log_2$  transformed. The fold change (E15.5/E12.5) of Aha-labeled proteins was calculated and averaged over biological replicates. Statistical analysis of transformed intensities was conducted using a two-tailed t test using Excel and corresponding p-values were  $\log_{10}$  transformed and visualized using GraphPad Prism 8.

#### Tissue Fractionation

Control E15.5 embryos, harvested from dams injected with PBS at E13.5 and E14.5, were fractionated using buffers of increasing stringency to selectively enrich for cytosolic (C), nuclear (N), membrane (M), cytoskeletal (CS) or ECM proteins as previously described,<sup>39,47</sup> with some modifications (Table S2). Embryos were mechanically homogenized with a TissueRuptor in C buffer (400 mg wet weight tissue in 500 μL buffer; Table S2), rotated end-over-end for 30 min at 4 °C, followed by centrifugation at  $14,000 \times g$ for 20 min. Supernatants were collected, snap frozen and stored at - 80 °C. The remaining pellet was resuspended in another 500 μL of C buffer and processed as previously described. The supernatant was snap frozen and stored at - 80 °C, to be combined with the first C fraction before subsequent processing. The pellet was then sequentially processed with N, M and CS buffers following the same protocol as described for the C buffer, with the exception that extractions using CS buffer were performed at RT. The remaining insoluble pellets (ECM) were snap frozen and stored at -80 °C.



## LC-MS/MS Analysis of Fractionated Tissue

Aliquots of C, N, M, and CS fractions were diluted twofold by combining 250  $\mu$ L lysate with 250  $\mu$ L 8 M urea containing 100 mM ammonium bicarbonate (final concentration 4 M urea). The ECM fraction was resuspended in 100 μL 8 M urea with 100 mM ammonium bicarbonate. Proteins in C and N fractions were reduced, alkylated, digested, desalted, and dried as described above for the Aha-enrichment study. M fractions were processed similarly, but were also cleaned with detergent removal columns prior to desalting. CS and ECM fractions were reduced and alkylated prior to deglycosylation with 0.1 U of chondroitinase ABC (Sigma-Aldrich) for 2 h at 37 °C, shaking at 1000 rpm. After deglycosylation, CS and ECM fractions were digested, processed with detergent removal columns, desalted, and dried. All samples were resuspended in 3% ACN with 0.1% FA and brought to 1  $\mu g/\mu L$ .

Samples of each fraction were analyzed on the QE HF as stated above, with each biological replicate representing a separate embryo (n=3). Raw data files were analyzed by MaxQuant as described above using the parameters as defined in Table S1. Additionally, samples were grouped by buffer fraction (C, N, M, CS, ECM) for label-free quantification (LFQ) analysis. Data was analyzed using Microsoft Excel and Prism for filtering and data visualization, respectively. Gene ontology (GO) terms and Reactome pathways on the 50 most abundant proteins in each fraction were analyzed using g:Profiler.  $^{19,42}$ 

# Temporal Study of Protein Turnover Using Aha

Time-mated females were injected with 0.1 mg/g Aha at E12.5, embryos were harvested 0, 3, 6, 12, 24, and 48 h after injection, snap frozen in liquid nitrogen and stored at -80 °C. Embryos were fractionated into different cellular compartments as described above and conjugated with biotin-alkyne in a CuAAC reaction with 25 mM iodoacetamide, 10 mM NaAsc, 50  $\mu$ M biotin-alkyne, 10 mM THPTA, 2 mM CuSO<sub>4</sub> and 20 mM AG for 2 h at RT. Reacted samples were precipitated with methanol-chloroform and air-dried protein pellets of C, N, M and CS fractions were resuspended in 2 × Laemmli buffer (BioRad) with 5%  $\beta$ -mercaptoethanol. ECM pellets were resuspended in 100 mM Tris-HCl (pH 7.6), 8% SDS, 0.1 M DTT, 1 × native Laemmli with 5%  $\beta$ -mercaptoethanol. All samples were then heated at 95 °C for 5 min and analyzed via western blotting as described above. Western blot images were analyzed using ImageJ (NIH, Bethesda, MD) to calculate the mean fluorescence intensities for each time point. A  $117 \times 816$  pixel region of interest (ROI) was generated that was slightly larger than the width of each lane. The sum of the intensity units in the ROI was measured using "Raw-IntDen." For each blot, the intensity at t=0 was used to normalize subsequent time points. Normalized intensity values for each fraction at each time point were plotted as a function of time, and the change in fluorescence intensity between time points were plotted and analyzed using Prism 8.0, n=3 biological replicates/blot.

#### RESULTS AND DISCUSSION

To determine the feasibility of enriching proteins that were newly synthesized within developing embryos, we first used biotin-alkyne to selectively enrich for Aha-labeled proteins. Time-mated C57BL/6 murine dams were injected subcutaneously with either 0.1 mg/g Aha or PBS (control) once a day for two days prior to harvesting at E15.5. Soluble proteins were isolated by homogenizing embryos in 0.3% SDS in PBS and the insoluble portion was removed by centrifugation. Western blot analysis of soluble lysates confirmed the feasibility of conjugating nascent proteins with biotin-alkyne in a CuAAC reaction, enriching with NeutrAvidin beads, and eluting Ahalabeled proteins from embryos (Fig. S1a). However, LC-MS/MS analysis of eluted proteins revealed avidin peptides dominated the MS/MS spectra, limiting the resolution by which Aha-labeled proteins can be resolved (Fig. S1b). The excess avidin was attributed to the use of harsh elution conditions, i.e. boiling in SDS, which disrupts the biotin-avidin interaction to elute biotinylated proteins. In addition, very few proteins were enriched in Aha-labeled samples as evidenced by Coomassie staining of eluted samples (Fig. S1a).

To overcome these limitations, diazo biotin-alkyne (DBA), a cleavable biotin linker was used (Fig. S2). The diazo group between the biotin and alkyne was cleaved by reducing with sodium dithionite (Na<sub>2</sub>S<sub>2</sub>O<sub>4</sub>) under mild conditions, preventing the elution of excess avidin (Fig. 1a).<sup>54</sup> Initial optimization experiments using cells cultured in vitro confirmed selective enrichment of Aha-labeled proteins. However, when more complex tissue samples were used (E15.5 embryos from dams injected with Aha or PBS), there was a substantial number of proteins also detected in unlabeled samples, suggesting nonspecific protein binding to NeutrAvidin beads. Several approaches were employed to eliminate nonspecific protein contamination including blocking beads with bovine serum albumin prior to lysate addition, incubating lysates with beads for shorter periods, and increasing the number and stringency of washes (data not shown). Nevertheless, none of these strategies resulted in reducing the level of eluted proteins in unlabeled samples.

We next tested the possibility that side reactions from the CuAAC (click) reaction conditions lead to nonspecific labeling of proteins with the diazo biotinalkyne linker. Soluble lysates from E15.5 embryos harvested from dams injected with PBS were reacted in the absence or presence of CuAAC and DBA reagents and were enriched with NeutrAvidin beads. A significant amount of unlabeled protein was eluted when using CuAAC and DBA, but not in the control or sample that was reacted with DBA only (Fig. S1c), suggesting that the alkyne linker conjugates to non-azide targets in CuAAC reaction conditions.

Ascorbate reduction of copper has been reported to produce dehydroascorbate as the oxidation product, which, along with other ascorbate byproducts, interacts with lysine and arginine side chains. 18,41 These interactions can result in the formation of several covalently cross-linked protein adducts, potentially leading to non-specific binding of unlabeled proteins to the beads. Aminoguanidine (AG), which is structurally similar to the guanidine group of arginine (Fig. S2a), was added to the click reaction mixture to investigate if it can reduce the nonspecific labeling by scavenging ascorbate byproducts.<sup>24</sup> Adding AG in the click reaction resulted in substantial reduction in nonspecific protein labeling without a comparable decrease in the amount of eluted proteins in the Aha sample (Fig. 1b). Furthermore, we found that higher concentrations of NaAsc increase background labeling, leading us to reduce the amount of this reagent in further reactions. Together, the addition of AG with the use of a cleavable linker provides us with a method that increases the identification of Aha-labeled proteins by reducing nonspecific binding in unlabeled samples as well as minimizing avidin contamination. For subsequent studies, 10 mM AG and 5 mM NaAsc were used in the click reaction.

To demonstrate this method could resolve differences in newly synthesized proteins within distinct time windows, dams were time-mated and injected so that Aha-labeling would occur between E10.5–E12.5 or E13.5–E15.5. Dams were injected with Aha or PBS (control) at t=0 and 24 h, and proteins were isolated from embryos at 48 h. Proteins from soluble lysates of E12.5 and E15.5 embryos were enriched using the workflow described in Fig. 1a, analyzed using LC–MS/MS and the raw intensity of proteins identified in Ahaand PBS-treated samples were compared (Fig. 2). Contaminants, reverse hits and proteins that had < 2 razor and unique peptides were filtered out, and a FDR of 0.01 was imposed. Approximately 50% of total proteins identified were found exclusively in Aha-



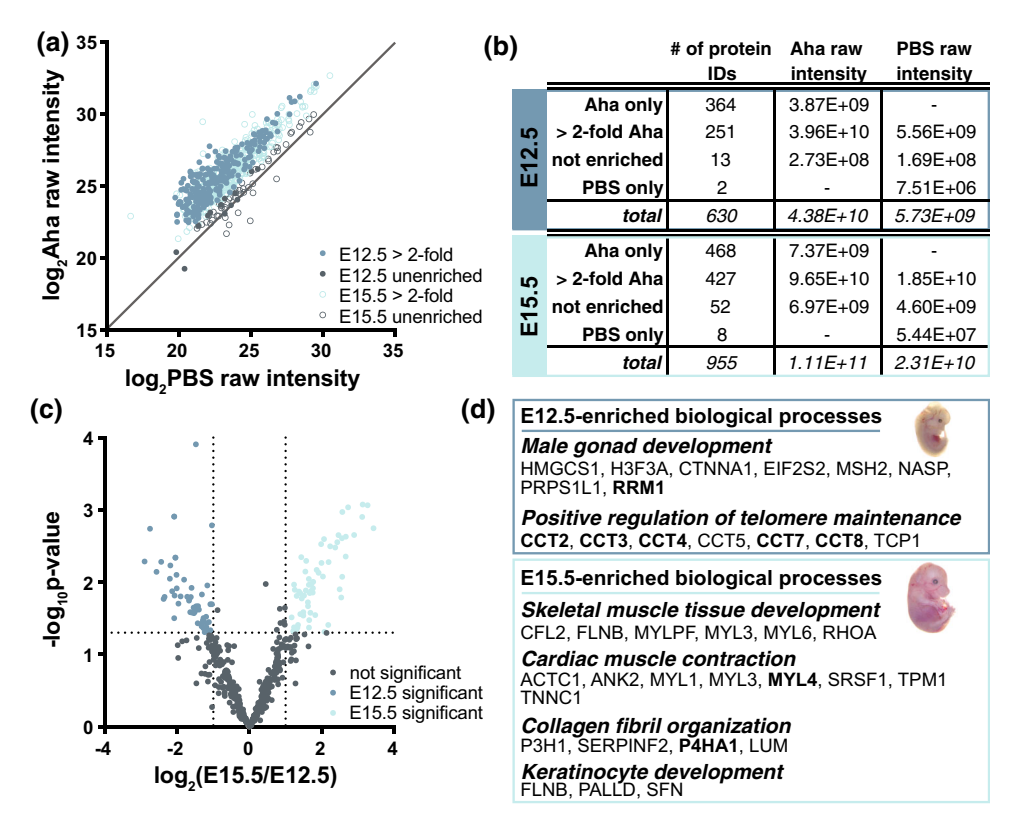


FIGURE 2. Enrichment of Aha-labeled proteins from different embryonic time points. Newly synthesized proteins isolated from E12.5 and E15.5 embryos were labeled with Aha as shown in Fig. 1a and the enriched proteins were analyzed using LC-MS/MS. (a) Scatter plot comparing the  $\log_2$  transformed intensity of proteins identified in both Aha and PBS revealed the substantial enrichment of Aha-labeled proteins at both E12.5 and E15.5. Each point is the average raw intensity of a single protein, n=3 biological replicates. See also Table S3. (b) Summary of protein IDs in Aha-labeled and PBS control samples. (c) Volcano plot of proteins identified in both E12.5 and E15.5 embryos. Proteins were considered significantly more abundant if there was > 2-fold difference and p < 0.05 between time points. Vertical lines indicate  $\pm 2$ -fold change, horizontal line indicates p = 0.05, calculated using a two-tailed  $\pm 2$ -fold compared with PBS for individual time points (see also Table S3). Proteins found at both time points, but > 2-fold at either E12.5 or E15.5 are indicated in bold.

treated embryos, and ~ 90% of proteins were > 2-fold enriched in Aha compared to PBS samples (Figs. 2a and 2b; Table S3). This degree of enrichment is in line with previous reports that used similar labeling strategies to investigate newly synthesized proteins in adult murine brains. 1,29 There was high correlation of protein intensity distributions between biological replicates, whereas there was low correlation between Aha and PBS samples (Fig. S3b). Analysis of Ahalabeled proteins revealed large contributions from cytosolic, nuclear and cytoskeletal proteins; however, very few matrisome and membrane proteins were identified (Fig. S3c).

Comparison of newly synthesized proteins isolated from the two embryonic time points revealed that 99 and 379 Aha-labeled proteins were exclusive to E12.5 and E15.5 lysates, respectively (Table S3). A volcano plot of the 516 Aha-labeled proteins that were common to both time points showed the subsets of proteins that were significantly more abundant (> 2-fold, p < 0.05) at E12.5 (54 proteins) and E15.5 (60 pro-

teins; Fig. 2c; Table S3). A Gene Ontology (GO) analysis was conducted to determine if Aha-enrichment could capture biological processes that pertained to these developmental time frames. Analysis of the newly synthesized proteins in Aha-labeled E12.5 samples identified biological process terms including *male gonad development* and *positive regulation of telomere maintenance* (Fig. 2d). Notably, genes that regulate sex determination are significantly upregulated around E11.0, and by E12.5 the transcriptomes between testes and ovaries are highly dimorphic.<sup>37</sup> In addition, maintaining telomere length is in line with previous studies that reported an increase in telomerase activity during the early stages of embryonic development.<sup>34,51</sup>

Analysis of the newly synthesized proteins in E15.5 samples generated biological process terms that were more indicative of later development, some of which are listed in Fig. 2d. Skeletal and cardiac muscle start rapidly differentiating after E11.5, 7,48 increasing the deposition of the contractile machinery such as the myosin light chain isoform MYL3, which is only ex-



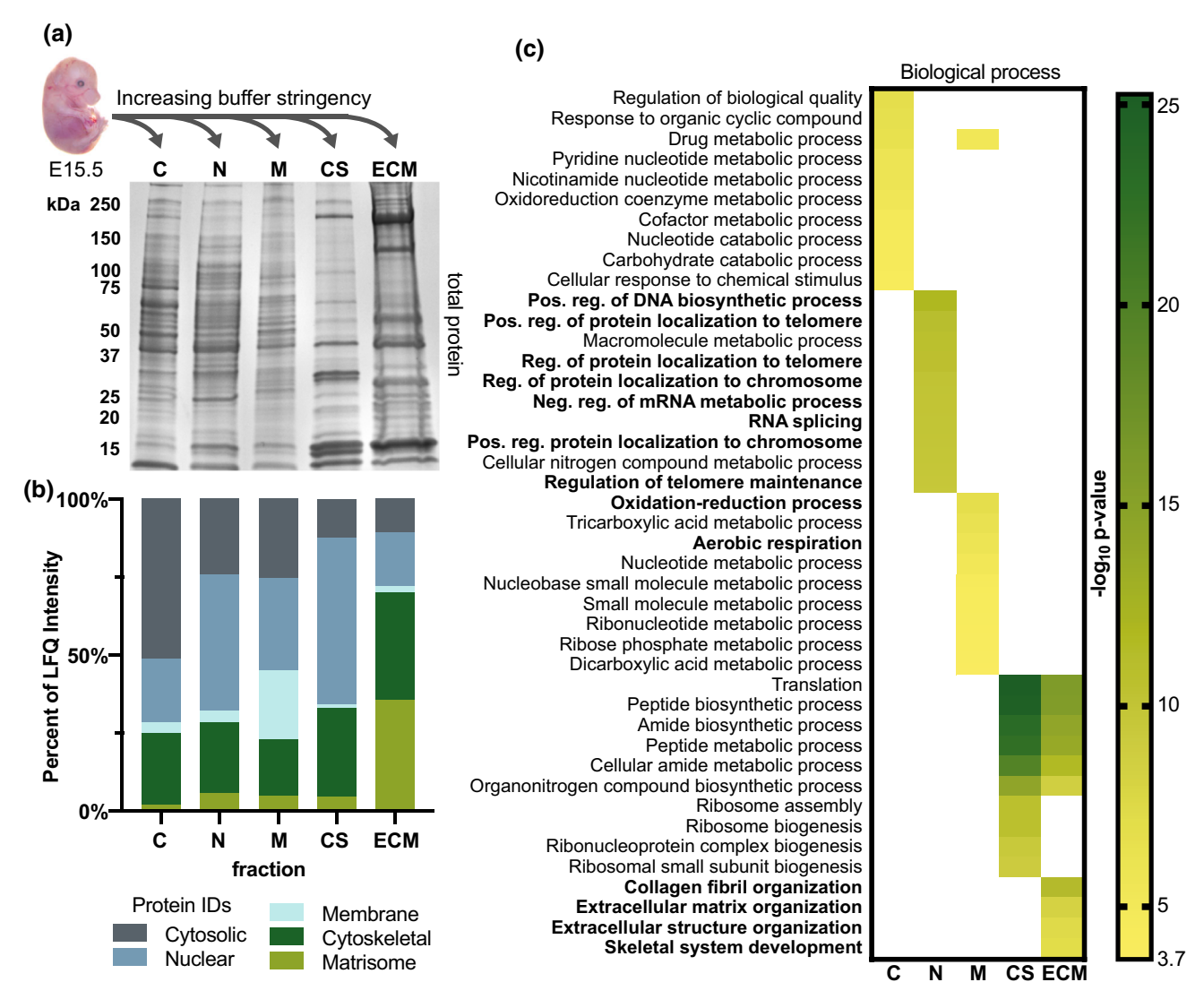


FIGURE 3. Fractionation of embryonic tissue into different cellular compartments. (a) Untreated E15.5 embryos were homogenized in buffers of increasing stringency to obtain cytosolic (C), nuclear (N), membrane (M), cytoskeletal (CS) and matrisome (ECM) fractions. (b) The distribution of intra- and extracellular proteins across the fractions, plotted as a percent of the average LFQ intensity of n = 3 embryos. See also Table S4. (c) Top 10 significantly enriched non-redundant GO biological process terms of the top 50 proteins from each fraction plotted as a function of their respective fractions. GO terms consistent with fraction isolation are in bold.

pressed in skeletal muscle around E15.5 (Fig. 2; Table S3).<sup>33</sup> To support and direct the growth of tissues, the ECM also needs to increase in density and become more organized.<sup>4,6</sup> Indeed, the expression of lumican (LUM), one of the small leucine-rich proteoglycans that regulate the assembly of type I collagen fibrils, increases dramatically between E11.5 and E15.5,<sup>55</sup> which is consistent with our identification of LUM only at E15.5 (Fig. 2; Table S3).

These studies only identified Aha-labeled proteins that were soluble in 0.3% SDS. Even if the proteins in the remaining insoluble portion were analyzed simultaneously with the 0.3% soluble proteins, it is unlikely that the number of IDs would be substantially

increased. A limitation of LC–MS/MS is that peptides of highly abundant proteins can mask the signal of those with similar properties but of lower abundance. One way to increase the number of protein IDs is to increase the time of the LC phase, effectively increasing the resolution; however, this also greatly increases cost. Alternatively, proteins can be analyzed in subsets depending on the biological question being asked. Examples include isolating by molecular weight or fractionating based on biochemical characteristics, such as lipid-soluble membrane proteins and the relatively insoluble ECM. <sup>39,40</sup>



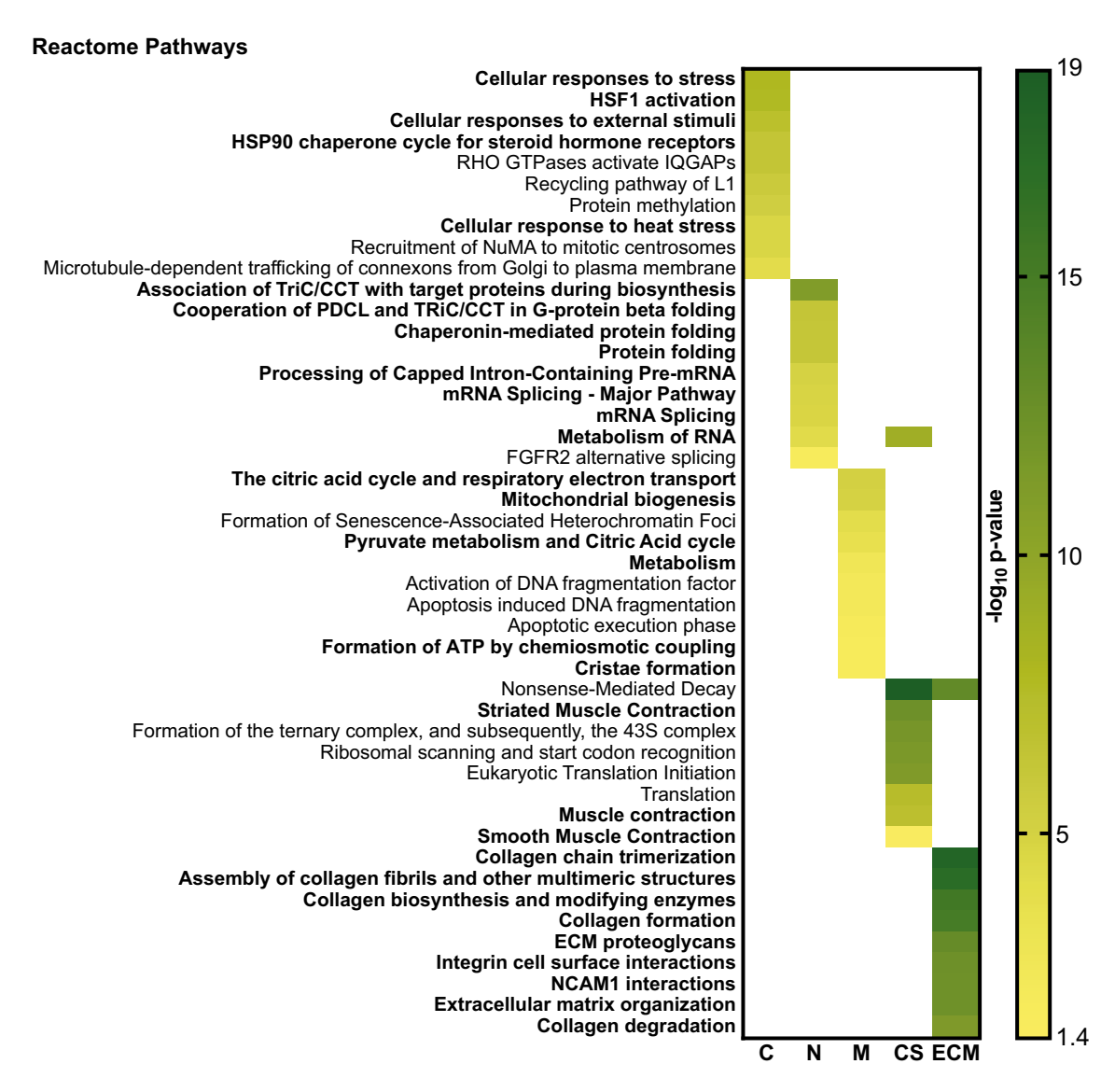


FIGURE 4. Reactome pathways reflect differential distribution of proteins across fractions. The top 10 significantly enriched, non-redundant Reactome terms based on the top 50 proteins from each fraction were determined for untreated E15.5 samples. Fraction-specific biological pathways discussed in text are indicated in bold.

Expanding the utility of *in vivo* ncAA labeling to identify newly synthesized proteins in different intraand extracellular compartments holds great potential for increasing the resolution of protein IDs in developmental model systems, but it is unclear if these methods, optimized on adult samples, <sup>12,14,20,23,38,47,52</sup> can be used on newly assembled embryonic tissues. To demonstrate the applicability of selectively fractionating different cellular compartments, unlabeled E15.5 embryos were homogenized using a protocol designed to isolate the cytosolic (C), nuclear (N), membrane (M), cytoskeleton (CS), and matrisome (ECM) fractions using buffers of increasing stringency (Table S2). <sup>38,47</sup> There is a clear distinction in the distribution of proteins of different molecular weight

across the fractions (Fig. 3a). To resolve compartment-specific protein dynamics, we performed LC-MS/MS on the different fractions from E15.5 embryos and annotated which cellular compartment the proteins were predominantly localized to based on the GO database (Fig. 3b; Table S4). Cytosolic, membrane and matrisome proteins were enriched in the appropriate fractions (C, M, and ECM respectively; Fig. 3b); whereas, nuclear and cytoskeletal proteins were more widely distributed. GO analysis of the 50 most abundant proteins in each fraction was performed. The top 10 significant biological process terms were plotted as a function of fraction and there was some enrichment of fraction-specific terms (bold; Fig. 3c).



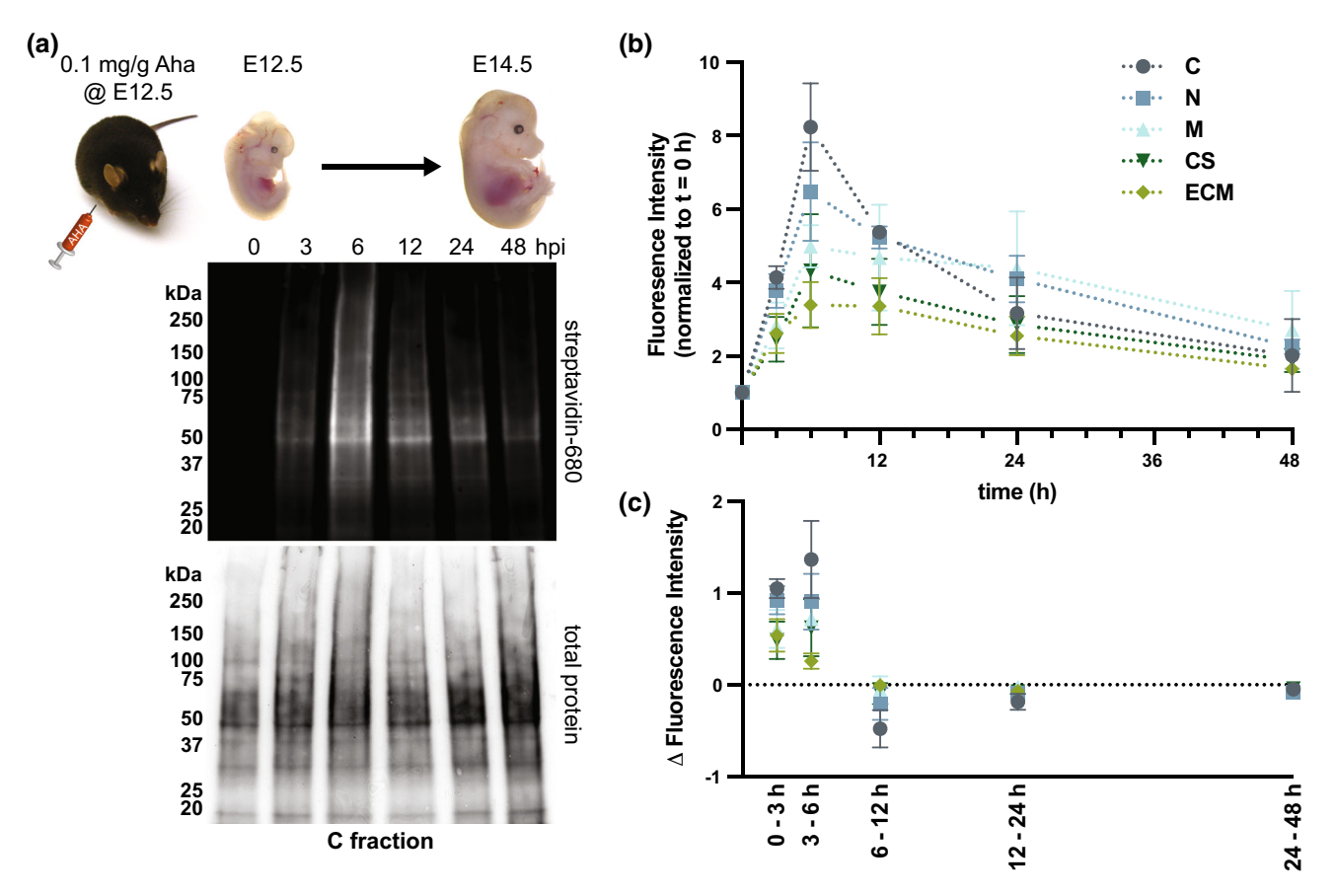


FIGURE 5. Persistence of Aha-labeled proteins in developing embryos. (a) Pregnant dams were injected one time with 0.1 mg/g Aha and embryos were harvested 0–48 h post injection (hpi). Proteins were isolated following Fig. 3a, fractions were clicked with biotin-alkyne and analyzed *via* western blotting (30  $\mu$ g/well). Shown is a representative image of the blot for the cytosolic (C) fraction (top). Ponceau S staining of the same membrane used to confirm equal loading (bottom). Representative images of the other fractions are shown in Figure S4. (b, c) Fluorescence intensity of western blot lanes were plotted as function of time and fraction, normalized to t = 0 (n = 3 biological replicates).

In contrast, terms for the same set of proteins derived from the Reactome pathway database<sup>19</sup> revealed trends that were more consistent with the types of proteins identified in each fraction (Fig. 4). Heat shock proteins and other responses to stress were represented by 5/10 of the most significant pathways in the C fraction. While these terms are typically associated with pathological processes, this large family of proteins that includes HSP90 and HSF1 also regulates normal embryonic development.<sup>45</sup> Pathways associated with the chaperonin family, a group of multimeric complexes that facilitate protein folding, were found in the N fraction (4/10). These proteins are found in both the nucleus and cytoplasm, <sup>13,21</sup> and have been shown, along with heat shock proteins, to be critical in response to stress as well as during organ growth.<sup>28</sup> In addition, another 4/10 terms in the N fraction are associated with mRNA metabolism. Interestingly, 6/10 terms in the M fraction are related to mitochondria, which can be attributed to this being a double membrane-bound organelle. The inner membrane forms

cristae that invaginate deep within the cell and contain the protein complexes of the respiratory system.<sup>30</sup> In the CS fraction, terms associated with muscle contraction made up 3/9 significant pathways, reflecting the large amount of cytoskeletal elements that striated and smooth muscle need to generate force.<sup>50</sup> Notably, the 9/10 terms in the ECM fraction are related to the matrisome and 5/10 are directly related to collagen metabolism, which is thought to be dynamic during embryogenesis.<sup>44</sup>

These results validate that fractionation protocols used on adult tissues are suitable for developing tissues, and the distribution of the Reactome terms is consistent with the cellular components expected to be identified in each fraction. The Reducing the complexity of individual samples will increase the overall identification of proteins by LC–MS/MS for more targeted studies. Specifically, we found LC–MS/MS analysis of the M fraction increased the overall intensity of membrane proteins identified when compared with whole embryo homogenate (Fig. S3c). Similarly, the



amount of matrisome components identified was increased when the ECM fraction was analyzed (Figs. 3 and S1a).

To investigate that protein turnover can be resolved within each cellular fraction, time-mated dams were injected once with 0.1 mg/g Aha at E12.5, and embryos were harvested at 0, 3, 6, 12, 24, and 48 h following injection. Lysates were fractionated, reacted with biotin-alkyne, and analyzed via western blotting using streptavidin-680. Overall, the highest degree of Aha-labeling was found 6 h after injection (Figs. 5 and S4). Between 3 and 24 h, the relative amount of labeling in different fractions varied considerably, as shown when the change in fluorescence intensity was plotted as a function of time (Figs. 5b and 5c). While measurements based on western blotting are semiquantitative, these results indicate that proteins of different solubility vary in turnover rate. Two-way ANOVA revealed that the effect of time and fraction were significant for both fluorescence intensity (p < 0.0001) for time and fraction; Fig. 5b) and change in fluorescence with respect to time (p < 0.0001 for time, p < 0.01 for fraction; Fig. 5c). Between E12.5 and E14.5, murine embryos increased in weight from  $95.0 \pm 9.2 \text{ mg}$  to  $275.3 \pm 20.8 \text{ mg}$  (average  $\pm \text{SD}$ ;  $N \ge 4$ ). Even with this large increase, Aha-labeled proteins were still present in all fractions 48 h after injection, which is consistent with a recent study demonstrating the lifetime of proteins in adult murine tissues for days.<sup>20</sup>

Overall, the results from this study set the stage for future investigations to combine the methods of Ahalabeling and enrichment with tissue fractionation to identify and quantify the key proteins involved with various developmental processes.

#### **CONCLUSION**

We previously demonstrated that *in vivo* ncAA labeling of murine proteins can be readily performed *via* intraperitoneal injection, allowing for labeling of newly synthesized proteins in a variety of tissues and at varying stages of development.<sup>8</sup> Here, we extend these results to show that subcutaneous injection of the Met analog Aha, in combination with an optimized enrichment protocol (Fig. 1), can be used to isolate newly synthesized proteins for LC–MS/MS identification with very little background relative to PBS injected controls. Approximately 50% of total protein IDs were found exclusively in Aha-labeled tissue, and 90% of proteins found in both Aha and PBS samples were enriched > 2-fold in the Aha-labeled samples

(Figs. 2 and S3). The proteins that were selectively enriched from E12.5 and E15.5 embryos were related to developmental processes occurring around each time point. In addition, we established the feasibility of using cellular fractionation, which enabled a broader investigation of intra- and extracellular proteins in developing embryos than standard isolation protocols. Reactome pathway analysis of LC-MS/MS data demonstrated that proteins identified in each fraction corresponded to the expected cellular compartment, i.e. cytosolic (C), nuclear (N), membrane (M), cytoskeleton (CS), and matrisome (ECM) fractions (Figs. 3 and 4). Finally, we combined in vivo ncAA labeling and cellular fractionation of embryos to investigate the turnover of proteins within each compartment. Significant labeling of newly synthesized proteins was observed by 3 h post-injection (Fig. 5a) and persisted for varying durations depending on cellular compartment (Figs. 5b and 5c).

Future efforts will combine our *in vivo* labeling approach (Fig. 1) with that of embryo fractionation (Fig. 5) and LC–MS/MS analysis to precisely determine the turnover rates of individual proteins. To do so, it will first be necessary to characterize the metabolism of Aha *in vivo*, which remains unknown. In addition, we will need to normalize for changes in mass/protein content that occur during development. Together, these approaches will provide insight into functional tissue assembly by enabling the mapping of protein synthesis and turnover at specific developmental time points in different cellular compartments.

## ELECTRONIC SUPPLEMENTARY MATERIAL

The online version of this article (https://doi.org/10. 1007/s12195-019-00592-1) contains supplementary material, which is available to authorized users.

#### ACKNOWLEDGMENTS

The authors would like to thank Victoria Hedrick and Uma Ayal at the Purdue Proteomics Core. This work was supported by the National Institutes of Health [R21 AR069248, R01 AR071359 and DP2 AT009833 to S.C.] The content is solely the responsibility of the authors and does not necessarily represent the official view of the NIH. This work was also supported by the National Science Foundation [CAREER 1752366 to TKU]. Any opinions, findings, and conclusions or recommendations expressed in this material are those of the authors and do not necessarily reflect the views of the National Science Foundation.



# CONFLICT OF INTEREST

Authors Aya Saleh, Kathryn Jacobson, Tamara Kinzer-Ursem, and Sarah Calve declare that they have no conflicts of interest.

#### ETHICAL STANDARDS

All experimental protocols involving animals were performed in compliance with established guidelines and all methods were approved by Purdue Animal Care and Use Committee (PACUC, protocols# 1209000723 and 1801001682). PACUC requires that all animal programs, procedures, and facilities at Purdue University to abide by the policies, recommendations, guidelines, and regulations of the USDA and the United States Public Health Service in accordance with the Animal Welfare Act and Purdue's Animal Welfare Assurance. Additionally, no human subjects research was conducted in this study.

## REFERENCES

- <sup>1</sup>Alvarez-Castelao, B., C. T. Schanzenbacher, C. Hanus, C. Glock, S. Tom Dieck, A. R. Dorrbaum, I. Bartnik, B. Nassim-Assir, E. Ciirdaeva, A. Mueller, D. C. Dieterich, D. A. Tirrell, J. D. Langer, and E. M. Schuman. Cell-typespecific metabolic labeling of nascent proteomes in vivo. Nat. Biotechnol. 35:1196-1201, 2017.
- <sup>2</sup>Ashburner, M., C. A. Ball, J. A. Blake, D. Botstein, H. Butler, J. M. Cherry, A. P. Davis, K. Dolinski, S. S. Dwight, J. T. Eppig, M. A. Harris, D. P. Hill, L. Issel-Tarver, A. Kasarskis, S. Lewis, J. C. Matese, J. E. Richardson, M. Ringwald, G. M. Rubin, and G. Sherlock. Gene ontology: tool for the unification of biology. The gene ontology consortium. Nat. Genet. 25:25-29, 2000.
- <sup>3</sup>Bagert, J. D., Y. J. Xie, M. J. Sweredoski, Y. Qi, S. Hess, E. M. Schuman, and D. A. Tirrell. Quantitative, time-resolved proteomic analysis by combining bioorthogonal noncanonical amino acid tagging and pulsed stable isotope labeling by amino acids in cell culture. Mol. Cell. Proteomics 13:1352–1358, 2014.
- <sup>4</sup>Birk, D. E., and P. Brückner. The Extracellular Matrix: An
- Overview. Berlin: Springer, pp. 77–115, 2011. <sup>5</sup>Borrmann, A., and J. C. M. van Hest. Bioorthogonal chemistry in living organisms. Chem. Sci. 5:2123-2134, 2014.
- <sup>6</sup>Brown, N. H. Extracellular matrix in development: insights from mechanisms conserved between invertebrates and vertebrates. Cold Spring Perspect. Biol. 3(12):a005082, 2011.
- <sup>7</sup>Buckingham, M., L. Bajard, T. Chang, P. Daubas, J. Hadchouel, S. Meilhac, D. Montarras, D. Rocancourt, and F. Relaix. The formation of skeletal muscle: from somite to limb. J. Anat. 202:59-68, 2003.
- <sup>8</sup>Calve, S., A. J. Witten, A. R. Ocken, and T. L. Kinzer-Ursem. Incorporation of non-canonical amino acids into the developing murine proteome. Sci. Rep. 6:32377, 2016.

- <sup>9</sup>Casas-Vila, N., A. Bluhm, S. Sayols, N. Dinges, M. Dejung, T. Altenhein, D. Kappei, B. Altenhein, J. Y. Roignant, and F. Butter. The developmental proteome of Drosophila melanogaster. Genome Res. 27:1273–1285, 2017.
- <sup>10</sup>Chen, X., S. Wei, Y. Ji, X. Guo, and F. Yang. Quantitative proteomics using SILAC: principles, applications, and developments. Proteomics 15:3175-3192, 2015.
- <sup>11</sup>Cox, J. Mann M (2008) MaxQuant enables high peptide identification rates, individualized p.p.b.-range mass accuracies and proteome-wide protein quantification. Nat. Biotechnol. 26:1367-1372, 2008.
- <sup>12</sup>Decaris, M. L., M. Gatmaitan, S. FlorCruz, F. Luo, K. Li, W. E. Holmes, M. K. Hellerstein, S. M. Turner, and C. L. Emson. Proteomic analysis of altered extracellular matrix turnover in bleomycin-induced pulmonary fibrosis. Mol. Cell. Proteomics 13:1741-1752, 2014.
- <sup>13</sup>Dekker, C., P. C. Stirling, E. A. McCormack, H. Filmore, A. Paul, R. L. Brost, M. Costanzo, C. Boone, M. R. Leroux, and K. R. Willison. The interaction network of the chaperonin CCT. EMBO J. 27:1827-1839, 2008.
- <sup>14</sup>Didangelos, A., X. Yin, K. Mandal, M. Baumert, M. Jahangiri, and M. Mayr. Proteomics characterization of extracellular space components in the human aorta. Mol. Cell Proteomics 9:2048-2062, 2010.
- <sup>15</sup>Dieterich, D. C., J. J. Hodas, G. Gouzer, I. Y. Shadrin, J. T. Ngo, A. Triller, D. A. Tirrell, and E. M. Schuman. In situ visualization and dynamics of newly synthesized proteins in rat hippocampal neurons. Nat. Neurosci. 13:897-905, 2010.
- <sup>16</sup>Dieterich, D. C., J. J. Lee, A. J. Link, J. Graumann, D. A. Tirrell, and E. M. Schuman. Labeling, detection and identification of newly synthesized proteomes with bioorthogonal non-canonical amino-acid tagging. Nat. Protoc. 2:532-540, 2007.
- <sup>17</sup>Dieterich, D. C., A. J. Link, J. Graumann, D. A. Tirrell, and E. M. Schuman. Selective identification of newly synthesized proteins in mammalian cells using bioorthogonal noncanonical amino acid tagging (BONCAT). Proc. Natl. Acad. Sci. USA 103:9482-9487, 2006.
- <sup>18</sup>Dunn, J. A., M. U. Ahmed, M. H. Murtiashaw, J. M. Richardson, M. D. Walla, S. R. Thorpe, and J. W. Baynes. Reaction of ascorbate with lysine and protein under autoxidizing conditions: formation of N epsilon-(carboxymethyl)lysine by reaction between lysine and products of autoxidation of ascorbate. Biochemistry 29:10964-10970, 1990.
- <sup>19</sup>Fabregat, A., S. Jupe, L. Matthews, K. Sidiropoulos, M. Gillespie, P. Garapati, R. Haw, B. Jassal, F. Korninger, B. May, M. Milacic, C. D. Roca, K. Rothfels, C. Sevilla, V. Shamovsky, S. Shorser, T. Varusai, G. Viteri, J. Weiser, G. Wu, L. Stein, H. Hermjakob, and P. D'Eustachio. The reactome pathway knowledgebase. Nucleic Acids Res. 46:D649–D655, 2018.
- <sup>20</sup>Fornasiero, E. F., S. Mandad, H. Wildhagen, M. Alevra, B. Rammner, S. Keihani, F. Opazo, I. Urban, T. Ischebeck, M. S. Sakib, M. K. Fard, K. Kirli, T. P. Centeno, R. O. Vidal, R. U. Rahman, E. Benito, A. Fischer, S. Dennerlein, P. Rehling, I. Feussner, S. Bonn, M. Simons, H. Urlaub, and S. O. Rizzoli. Precisely measured protein lifetimes in the mouse brain reveal differences across tissues and subcellular fractions. Nat. Commun. 9:4230, 2018.
- <sup>21</sup>Frydman, J. Folding of newly translated proteins in vivo: the role of molecular chaperones. Annu. Rev. Biochem. 70:603-647, 2001.



<sup>22</sup>Geiger, T., A. Velic, B. Macek, E. Lundberg, C. Kampf, N. Nagaraj, M. Uhlen, J. Cox, and M. Mann. Initial quantitative proteomic map of 28 mouse tissues using the SILAC mouse. *Mol. Cell. Proteomics* 12:1709–1722, 2013.

<sup>23</sup>Hill, R. C., E. A. Calle, M. Dzieciatkowska, L. E. Niklason, and K. C. Hansen. Quantification of extracellular matrix proteins from a rat lung scaffold to provide a molecular readout for tissue engineering. *Mol. Cell. Proteomics* 14:961–973, 2015.

<sup>24</sup>Hong, V., S. I. Presolski, C. Ma, and M. G. Finn. Analysis and optimization of copper-catalyzed azide-alkyne cycloaddition for bioconjugation. *Angew. Chem. Int. Ed. Engl.* 48:9879–9883, 2009.

<sup>25</sup>Kessels, M. Y., L. F. Huitema, S. Boeren, S. Kranenbarg, S. Schulte-Merker, J. L. van Leeuwen, and S. C. de Vries. Proteomics analysis of the zebrafish skeletal extracellular matrix. *PLoS ONE* 9:e90568, 2014.

<sup>26</sup>Kiick, K. L., E. Saxon, D. A. Tirrell, and C. R. Bertozzi. Incorporation of azides into recombinant proteins for chemoselective modification by the Staudinger ligation. *Proc. Natl. Acad. Sci. USA* 99:19–24, 2002.

<sup>27</sup>Kiick, K. L., R. Weberskirch, and D. A. Tirrell. Identification of an expanded set of translationally active methionine analogues in *Escherichia coli. FEBS Lett.* 502:25–30, 2001.

<sup>28</sup>Kim, A. R., and K. W. Choi. TRiC/CCT chaperonins are essential for organ growth by interacting with insulin/TOR signaling in Drosophila. *Oncogene* 38(24):4739, 2019.

- <sup>29</sup>Krogager, T. P., R. J. Ernst, T. S. Elliott, L. Calo, V. Beranek, E. Ciabatti, M. G. Spillantini, M. Tripodi, M. H. Hastings, and J. W. Chin. Labeling and identifying cell-specific proteomes in the mouse brain. *Nat. Biotechnol.* 36:156–159, 2018.
- <sup>30</sup>Kuhlbrandt, W. Structure and function of mitochondrial membrane protein complexes. *BMC Biol.* 13:89, 2015.
- <sup>31</sup>Li, X., C. Zhang, T. Gong, X. Ni, J. Li, D. Zhan, M. Liu, L. Song, C. Ding, J. Xu, B. Zhen, Y. Wang, and J. Qin. A time-resolved multi-omic atlas of the developing mouse stomach. *Nat. Commun.* 9:4910, 2018.
- <sup>32</sup>Lucitt, M. B., T. S. Price, A. Pizarro, W. Wu, A. K. Yocum, C. Seiler, M. A. Pack, I. A. Blair, G. A. Fitzgerald, and T. Grosser. Analysis of the zebrafish proteome during embryonic development. *Mol. Cell. Proteomics* 7:981–994, 2008.
- <sup>33</sup>Lyons, G. E., M. Ontell, R. Cox, D. Sassoon, and M. Buckingham. The expression of myosin genes in developing skeletal muscle in the mouse embryo. *J. Cell. Biol.* 111:1465–1476, 1990.
- <sup>34</sup>Martin-Rivera, L., E. Herrera, J. P. Albar, and M. A. Blasco. Expression of mouse telomerase catalytic subunit in embryos and adult tissues. *Proc. Natl. Acad. Sci USA* 95:10471–10476, 1998.
- <sup>35</sup>McClatchy, D. B., M. Q. Dong, C. C. Wu, J. D. Venable, and J. R. Yates, 3rd. 15 N metabolic labeling of mammalian tissue with slow protein turnover. *J. Proteome Res.* 6:2005–2010, 2007.
- <sup>36</sup>McClatchy, D. B., Y. Ma, C. Liu, B. D. Stein, S. Martinez-Bartolome, D. Vasquez, K. Hellberg, R. J. Shaw, and J. R. Yates, 3rd. Pulsed azidohomoalanine labeling in mammals (PALM) detects changes in liver-specific LKB1 knockout mice. *J. Proteome Res.* 14:4815–4822, 2015.
- <sup>37</sup>Munger, S. C., A. Natarajan, L. L. Looger, U. Ohler, and B. Capel. Fine time course expression analysis identifies

- cascades of activation and repression and maps a putative regulator of mammalian sex determination. *PLoS Genet*. 9:e1003630, 2013.
- <sup>38</sup>Naba, A., K. R. Clauser, S. Hoersch, H. Liu, S. A. Carr, and R. O. Hynes. The matrisome: in silico definition and in vivo characterization by proteomics of normal and tumor extracellular matrices. *Mol. Cell. Proteomics* 11:M111-014647, 2012.
- <sup>39</sup>Naba, A., K. R. Clauser, and R. O. Hynes. Enrichment of extracellular matrix proteins from tissues and digestion into peptides for mass spectrometry analysis. *JoVE* 101:e53057, 2015.
- <sup>40</sup>Paulo, J. A. Sample preparation for proteomic analysis using a GeLC-MS/MS strategy. J. Biol. Methods 3:e45, 2016.
- <sup>41</sup>Reihl, O., M. O. Lederer, and W. Schwack. Characterization and detection of lysine-arginine cross-links derived from dehydroascorbic acid. *Carbohydr. Res.* 339:483–491, 2004
- <sup>42</sup>Reimand, J., T. Arak, P. Adler, L. Kolberg, S. Reisberg, H. Peterson, and J. Vilo. g:Profiler-a web server for functional interpretation of gene lists (2016 update). *Nucleic Acids Res.* 44:W83–89, 2016.
- <sup>43</sup>Rostovtsev, V. V., L. G. Green, V. V. Fokin, and K. B. Sharpless. A stepwise huisgen cycloaddition process: copper(1)-catalyzed regioselective "ligation" of azides and terminal alkynes. *Angew. Chem. Int. Ed. Engl.* 41:2596–2599, 2002.
- <sup>44</sup>Rozario, T., and D. W. DeSimone. The extracellular matrix in development and morphogenesis: a dynamic view. *Dev. Biol.* 341:126–140, 2010.
- <sup>45</sup>Rupik, W., K. Jasik, J. Bembenek, and W. Widłak. The expression patterns of heat shock genes and proteins and their role during vertebrate's development. *Comp. Biochem. Phys. A* 159:349–366, 2011.
- <sup>46</sup>Saleh, A. M., K. M. Wilding, S. Calve, B. C. Bundy, and T. L. Kinzer-Ursem. Non-canonical amino acid labeling in proteomics and biotechnology. *J. Biol. Eng.* 13:43, 2019.
- <sup>47</sup>Schiller, H. B., I. E. Fernandez, G. Burgstaller, C. Schaab, R. A. Scheltema, T. Schwarzmayr, T. M. Strom, O. Eickelberg, and M. Mann. Time- and compartment-resolved proteome profiling of the extracellular niche in lung injury and repair. *Mol. Syst. Biol.* 11:819, 2015.
- <sup>48</sup>Siedner, S., M. Kruger, M. Schroeter, D. Metzler, W. Roell, B. K. Fleischmann, J. Hescheler, G. Pfitzer, and R. Stehle. Developmental changes in contractility and sarcomeric proteins from the early embryonic to the adult stage in the mouse heart. *J. Physiol.* 548:493–505, 2003.
- <sup>49</sup>Sun, L., M. M. Bertke, M. M. Champion, G. Zhu, P. W. Huber, and N. J. Dovichi. Quantitative proteomics of Xenopus laevis embryos: expression kinetics of nearly 4000 proteins during early development. Sci. Rep. 4:4365, 2014.
- proteins during early development. *Sci. Rep.* 4:4365, 2014. <sup>50</sup>Sweeney, H. L., and D. W. Hammers. Muscle contraction. *Cold Spring Perspect. Biol.* 10(2):a023200, 2018.
- <sup>51</sup>Varela, E., R. P. Schneider, S. Ortega, and M. A. Blasco. Different telomere-length dynamics at the inner cell mass versus established embryonic stem (ES) cells. *Proc. Natl. Acad. Sci. USA* 108:15207–15212, 2011.
- <sup>52</sup>Warren, C. M., D. L. Geenen, D. L. Helseth, Jr, H. Xu, and R. J. Solaro. Sub-proteomic fractionation, iTRAQ, and OFFGEL-LC-MS/MS approaches to cardiac proteomics. *J. Proteomics* 73:1551–1561, 2010.



<sup>53</sup>Williams, C., K. P. Quinn, I. Georgakoudi, and L. D. Black, 3rd. Young developmental age cardiac extracellular matrix promotes the expansion of neonatal cardiomyocytes in vitro. *Acta Biomater*. 10:194–204, 2014.

<sup>54</sup>Yang, Y. Y., M. Grammel, A. S. Raghavan, G. Charron, and H. C. Hang. Comparative analysis of cleavable azobenzene-based affinity tags for bioorthogonal chemical proteomics. *Chem. Biol.* 17:1212–1222, 2010.

<sup>55</sup>Ying, S., A. Shiraishi, C. W. Kao, R. L. Converse, J. L. Funderburgh, J. Swiergiel, M. R. Roth, G. W. Conrad, and W. W. Kao. Characterization and expression of the mouse lumican gene. *J. Biol. Chem.* 272:30306–30313, 1997.

**Publisher's Note** Springer Nature remains neutral with regard to jurisdictional claims in published maps and institutional affiliations.

